IEEE Access
Multidisciplinary | Rapid Review | Open Access Journal

Received May 20, 2020, accepted July 13, 2020, date of current version August 18, 2020.

Digital Object Identifier 10.1109/ACCESS.2020.3012984

Multi-Frequency Data Fusion for Attitude Estimation Based on Multi-Layer Perception and Cubature Kalman Filter

XUEMEI CHEN, ZHENG XUELONG, ZIJIA WANG, MENGXI LI, YANGJIAXIN OU, AND SUN YUFAN

Intelligent Vehicle Research Center, School of Mechanical Engineering, Beijing Institute of Technology, Beijing 100081, China

Corresponding author: Xuemei Chen (chenxue781@126.com)

This work was supported in part by the Youth Science Fund under Grant 51705021, in part by the Automobile Industry Joint Fund under Grant U1764261, in part by the National Natural Science Foundation of China, Beijing Municipal Science and Technology Project under Grant Z191100007419010, and in part by the Key Laboratory for New Technology Application of Road Conveyance of Jiangsu Province under Grant BM20082061706.

ABSTRACT This paper proposes multi-frequency inertial and visual data fusion for attitude estimation. The proposed strategy is based on the locally weighted linear regression (LWLR), multi-layer perception (MLP), and cubature Kalman filter (CKF). First, we analyze the discrepant-frequency and the attitude divergence problems. Second, we construct the filter equation for the visual and inertial data and attitude differential equation for inertial-only data, which are used to estimate the attitude in time series. Third, we employ LWLR to compute the vision discrepancies between actual vision data and fitted vision data. The vision discrepancy is used as the input of MLP training. In MLP, the discrepancy is used as weights of the sums through the activation function of the hidden layer. To address the divergence problem, which is inherent in a multi-frequency fusion, the MLP is utilized to compensate for the inertial-only data. Finally, experimental results on different environments of pseudo-physical simulations show the superior performance of the proposed method in terms of the accuracy of attitude estimation and divergence capability.

INDEX TERMS Attitude estimation, multi-frequency, locally weighted linear regression, multi-layer perception, cubature Kalman filter.

I. INTRODUCTION

Accurate and stable attitude estimation is an essential element in broad applications such as positioning, navigation, tracking, and augmented reality [1]–[3]. In the helmet tracking system [4], [5], robot control, and positioning [6], [7], attitude measuring method [8] obtains the spatial attitude of the object by outputting pitch, yaw, and roll angles. The typical approaches are inertial measurement and vision measurement. Inertial sensors are low cost with high sampling-frequency [9]–[11]. However, the measuring error of inertial sensors is rapidly accumulated over time because of the bias drift phenomenon and unstable calibration coefficient [12]–[14]. The visual sensor is stable, while the sampling-frequency is low compared with inertial sensors. Thus, the visual sensor is hard to track fast-moving objects. In order to overcome the limitation of a single sensor and ensure accuracy and stability, an integrated measurement system was actively exploited in attitude estimation. In this paper, we integrate inertial and vision sensors, utilizing the complementary advantages of them. The integration of inertial and vision sensors improves the attitude estimation in terms of stability and estimation accuracy.

Non-linear Kalman filter was used to integrate inertial and vision data in EKF [15], UKF [16], and CKF [17], [18]. The EKF [15] modeled the system by the first-order linearization. Thus, the EKF provided poor performance for non-linear dynamic systems [19]. The UKF [16] addressed the non-linear state estimation based on the controlling theory, achieving preciser accuracy than EKF. The CKF [17], [18] realized the non-linear filter under the Bayesian filtering framework, providing more stable performance.

In the CKF, the sampling-frequency discrepancy phenomenon exists between vision and inertial data [20], which

The associate editor coordinating the review of this manuscript and approving it for publication was Hossein Rahmani.

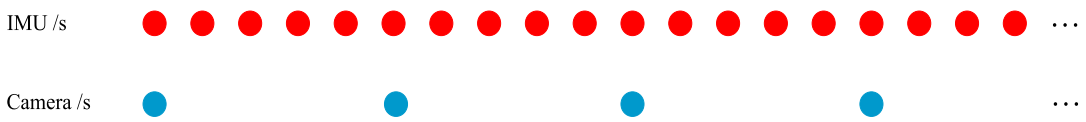

FIGURE 1. The discrepant frequency of sampling between IMU and camera.

is decided by vision sensors and inertial sensors self-characteristics. The performance of the attitude estimation is decreased by the discrepancy between vision data and inertial data. The performance degradation is inevitable in the inter-sampling of slow vision data. The differential operation causes the divergence phenomenon during invalid vision data intervals, where only inertial data is available. An artificial neural network (ANN) [21] was employed to enhance the attitude precision by using machine learning. Attitude determination (AD) model and partial ambiguity resolution (PAR) [22] were developed to meet the required reliability of attitude estimation. Also, they obtained an optimal balance between reliability and accuracy. SVD and UKF were fused with non-linear measurements [23], [24]. These methods provided accurate and stable results but were limited in multi-frequency. In case that vision data is unavailable, the accuracy of attitude estimation is decreased due to the discrepancy of sampling-frequency.

In order to address the problem, a data fusion method is proposed based on the combined LWLR and MLP with CKF. The contributions of this paper can be concluded as:

(1) The filter equation is constructed for the visual and inertial data and attitude differential equation for inertial-only data, which are used to estimate the attitude in time series;

(2) LWLR is employed to compute the vision discrepancies between actual vision data and fitted vision data.

The proposed method reduces the effect of the discrepant sampling-frequency, and consequently, the attitude divergence between inertial and vision data. The remainder of the paper is organized as follows. The problem exposition and system modeling are given in Section II. The proposed method is described in detail in Section III. The experiment and comparison with other methods are given in Section IV. In Section V, this paper is summarized and concluded.

A. MATERIALS AND METHODS

B. PROBLEM EXPOSITION

Different sampling-frequency inevitably causes the mismatch problem in the integrated system of inertial and vision sensors. The integrated attitude estimation system employs a camera sensor and a gyroscope sensor for capturing the vision and inertial data, respectively. Typically, the sampling-frequency of gyroscope is hundreds of Hertz, while that of a camera is dozens of Hertz. The discrepancy of sampling-frequency is depicted in Fig. 1.

The discrepant-frequency problem causes divergence of inertial and vision integrated attitude estimation. CKF fuses inertial and vision data to dispose of the non-linear problem. Inertial vectors are the input of the filter, and vision vectors are outputs computed from the filter. The non-linear filter is composed of state and measurement vectors, which is defined as follows.

$$\begin{cases} \mathrm{x}_k = f(x_{k-1}, u_{k-1}) + w_{k-1} \\ z_k = H_k x_k + v_k, \end{cases} \tag{1}$$

where x_k and u_{k-1} represent a state vector and a control vector from the angular velocity of the gyroscope, respectively. z_k is an observation vector from the vision sensor. Note that u_{k-1} is high-frequency and z_k is low-frequency. H_k represents the measurement matrix, w_{k-1} and v_k indicate the Gaussian random noises with different covariances.

Inertial and vision data are fused to estimate the optimal attitude. However, during the invalid vision data intervals, much inertial gyroscope data is still there. We employ a differential equation to update angles of attitude, which ensures the high frequency of estimated attitude. Specifically, the formula is given in the following.

$$\mathbf{q}(k+1) = (\cos(\frac{|\omega|\,\Delta t}{2})\mathbf{I} + 2\frac{\sin\left(\frac{|\omega|\Delta t}{2}\right)}{|\omega|}\mathbf{\Omega}(\omega))\mathbf{q}(k), \tag{2}$$

where $\mathbf{q}$ and $\mathbf{I}$ represent a rotation quaternion and a unit matrix, respectively. $\omega = \left[\omega_x \omega_y \omega_z\right]^T$ is angular velocity. Moreover, $\mathbf{\Omega}(\omega)$ is defined as follows:

$$\mathbf{\Omega}(\omega) = \frac{1}{2}\begin{bmatrix} 0 & -\omega_x & -\omega_y & -\omega_z \\ \omega_x & 0 & \omega_z & -\omega_y \\ \omega_y & -\omega_z & 0 & \omega_x \\ \omega_z & \omega_y & -\omega_x & 0 \end{bmatrix}. \tag{3}$$

During solving (2) to update the attitude, the measurement errors are accumulated over time because of the gyroscope bias error drift. The problem is mainly caused by the MEMS gyroscope sensor has non-negligible bias and noises. Furthermore, such bias and noise are accumulated due to the integral operation. Thus, we cannot guarantee that the inter-sampling of vision data is converged, especially when the interval is long.

C. SYSTEM MODELING

The proposed attitude estimation system is composed of the inertial and vision modules, as depicted in Fig. 2. In the vision module, visual attitude is obtained by the image processing module with the stereoscopic target with four feature points as an input. In the inertial module, attitude velocity is obtained

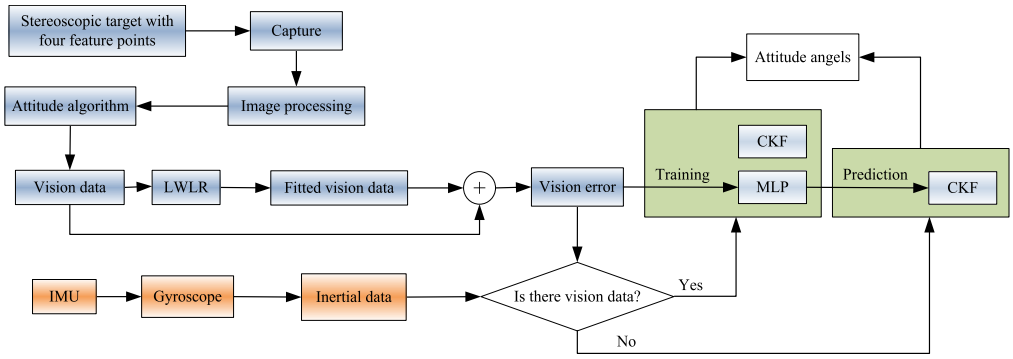

FIGURE 2. The proposed attitude estimation model with inertial and vision data.

by the built-in gyroscope of the IMU. When both inertial and vision data are available, they are fused by CKF. However, when the vision data is unavailable, the observation noise and Kalman gain approach to infinity and zero, respectively. As a result, the system only utilizes the inertial module and results in divergence.

II. THE ENHANCED FUSION METHOD BASED ON LWLR, MLP, AND CKF

A. BASIC FILTER PROCESS OF SKF ALGORITHM

In order to address the discrepant-frequency problem, an enhanced fusion method is proposed based on LWLR, MLP, and CKF. CKF utilizes a set of cubature points to approximate the probability distribution of non-linear function in moderate computation complexity. Also, the complex parameter selection process is not required in CKF since the unique weights and cubature points are selected according to the dimension of the state vector. The filtering process is described in detail as follows.

1) COMPUTATION OF VOLUME POINT

$$\xi_i = \sqrt{n}\,[1]_i\,, \tag{4}$$

$$\omega_i = \frac{1}{2n}, \quad i = 1, 2, \ldots, 2n, \tag{5}$$

$$\omega_{i,k|k-1} = \sqrt{P_{k-1|k-1}\xi_i} + \hat{x}_{k-1|k-1}, \tag{6}$$

where [1] is a symmetric matrix whose dominant diagonal lines are 1. A subscript i indicates the i^{th} column.

2) UPDATE OF TIME

The estimated attitude and covariance matrix are defined as (7) and (8), respectively, where k is the time.

$$\hat{x}_{k|k-1} = \frac{1}{2n}\sum_{i=1}^{2n} X_{i,k|k-1} \tag{7}$$

$$P_{k|k-1} = \frac{1}{2n}\sum_{i=1}^{2n} X_{i,k|k-1}X_{i,k|k-1}^T - \hat{x}_{k|k-1}\hat{x}_{k|k-1}^T \tag{8}$$

3) UPDATE OF MEASUREMENT

the volume point is computed as (9):

$$X_{i,k|k-1} = \sqrt{P_{k|k-1}\xi_i} + \hat{x}_{k|k-1} \tag{9}$$

The volume point is then propagated using measurement equation as follows:

$$Z_{i,k|k-1} = h(X_{i,k|k-1}) \tag{10}$$

$$\hat{z}_{k|k-1} = \frac{1}{2n}\sum_{i=1}^{2n} Z_{i,k|k-1} \tag{11}$$

The predicted measurement and covariance matrix are defined as follows, where k is the time.

$$P_{xz,k|k-1} = \sum_{i=1}^{2n} \omega_i X_{i,k|k-1}Z_{i,k|k-1}^T - \hat{x}_{k|k-1}\hat{z}_{k|k-1}^T \tag{12}$$

$$P_{zz,k|k-1} = \sum_{i=1}^{2n} \omega_i Z_{i,k|k-1}Z_{i,k|k-1}^T - \hat{x}_{k|k-1}\hat{z}_{k|k-1}^T \tag{13}$$

Kalman filter gain is computed as follows:

$$K_k = P_{xz,k|k-1}P_{zz,k|k-1}^{-1} \tag{14}$$

The estimated attitude and the covariance of the error of attitude are defined as follows.

$$\hat{x}_{k|k} = \hat{x}_{k|k-1} + K_k(z_k - \hat{x}_{k|k-1}) \tag{15}$$

$$P_{k|k} = P_{k|k-1} - K_k P_{zz,k|k-1}K_k^T \tag{16}$$

B. LOCALLY WEIGHTED LINEAR REGRESSION ALGORITHM

LWLR is a linear regression, which fits data by solving unbiased estimates of minimum mean squared error. Each point near the predicted point is given a certain weight in the LWLR algorithm. When predicting, only some samples similar to the experimental data are used to calculate regression coefficients. The points near the predicted points have high weights, and the weights decrease with the increase of distance. In this paper, the LWLR algorithm uses the Gauss kernel function to

give higher weights to the stores near the measuring points. The weight expression of the LWLR algorithm is as follows:

$$\omega(i) = \exp(\frac{(x^{(i)} - x)^2}{-2k^2}), \tag{17}$$

where w is the weight of the points near the measured points, and x means the points to be measured. k is a parameter that controls the rate of weight variation. k is set to 1 in the proposed LWLR algorithm to avoid over-fitting (when k is small) and under-fitting (when k is large).

LWLR algorithm can avoid the problem of under-fitting, because the influence of noise can be mitigated by weight, and more accurate data can be obtained. LWLR relies less on feature selection, so a simple linear model can be used to train a better fitting model. Each prediction is based on the original training samples to learn and calculate the weights again so that the data itself is adaptive, and the prediction accuracy is high.

C. MLP ALGORITHM

MLP is a forward-structured neural network, which is composed of one or multiple hidden layers with input and output layers. The network shows a high degree of connectivity, and its strength is determined by the weight of the network. MLP overcomes the weakness that perceptron cannot recognize linear non-separable data. Each neuron is composed of multiple inputs and outputs. Each output is computed with weights, bias, and activation function. The sigmoid function is adopted as the activation function in hidden layers, which is defined as follows.

$$sigmoid(x) = \frac{1}{1 + e^{-x}} \tag{18}$$

MLP is composed of several simple processing units, and it is executable in parallel. MLP stores weights and biases through its network structure, which makes the network have benign fault tolerance. The weights are learned with a training dataset in MLP, which reflects its strong learning ability and adaptability to the environment. Fig. 3 shows a typical three layers of network structure.

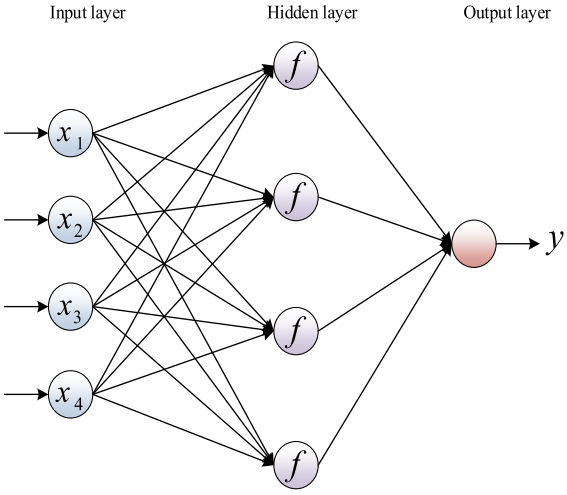

FIGURE 3. Three layers of MLP structure.

D. THE ENHANCED FUSION METHOD BASED ON LWLR, MLP, AND CKF

In order to address the discrepant-frequency problem, the enhanced fusion method is proposed based on LWLR, MLP, and CKF algorithms for the attitude estimation system. MLP predicts the vision error, which is trained using the discrepancy in vision data. The discrepancy is calculated by the subtraction of the visual sensory data and the fitted data obtained by LWLR. The predicted vision error is used to compensate for the attitude when the vision data is unavailable. The fitted vision data is obtained by the LWLR, where each point near the vision data is given a certain weight. Thus, the LWLR algorithm can reduce the impact of noise data on the overall data.

In the hidden layer, the vision error is used to weight the sum of the output layer by the kernel function. In the prediction process, the MLP neural network model predicts the vision data. CKF generates the attitude angles by fusing the gyroscope inertial data and the predicted vision data from MLP. CKF is employed for data fusion when both inertial and vision data are available. During the interval of invalid vision data, the combination of MLP and CKF estimates the attitude. Through such a complementary way, an accurate attitude can be stably estimated.

Figs. 4 and 5 show the specific processing diagrams of MLP during training and prediction processes, respectively. Fig. 4 shows how MLP trains when the vision sensor is available. The vision error is the input of MLP, and the sigmoid function is employed to convey the error to the output layer for the weighting sum. The estimated attitude is obtained by fusing the inertial data and actual vision data. The prediction flow of MLP during the interval of invalid vision data is shown in Fig. 5. Actual vision error is used to train MLP, and the trained MLP predicts the vision error. Inertial data from gyroscope are corrected by MLP prediction result to provide final attitude angles.

The reliably estimated attitude is obtained by integrating data based on MLP and CKF. The adverse effect of discrepant sampling-frequency can be lessen by the proposed method. The divergence problem led by different sampling-frequency is reformed and the precision of estimated attitude is improved.

III. EXPERIMENT AND COMPARISON

We evaluate the performance of the proposed method on the semi-physical simulation platform for attitude estimation system (Fig. 6). Following a platform proposed in [25], the camera was fixed onto the bracket, while IMU and the target were fixed onto the turntable. Four infrared LEDs are located onto the target. Only four feature points were used to reduce the workload of computational processing while improving the efficiency of data fusion. The angular velocity and the vision data were respectively collected with an external PC

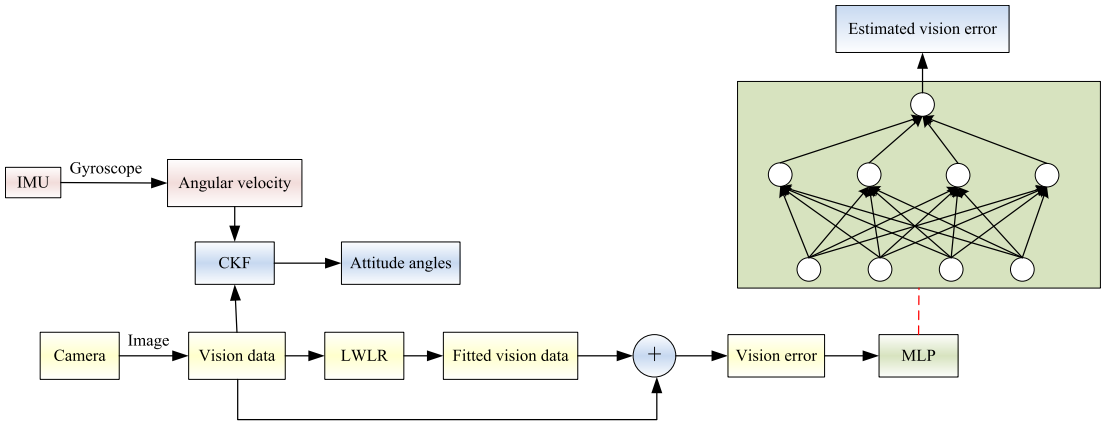

FIGURE 4. Processing of MLP training with vision error.

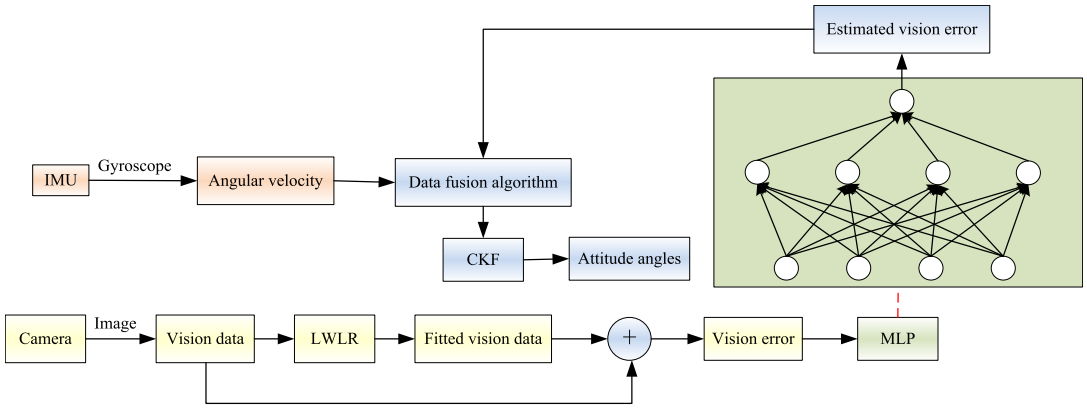

FIGURE 5. Processing of MLP prediction with vision error.

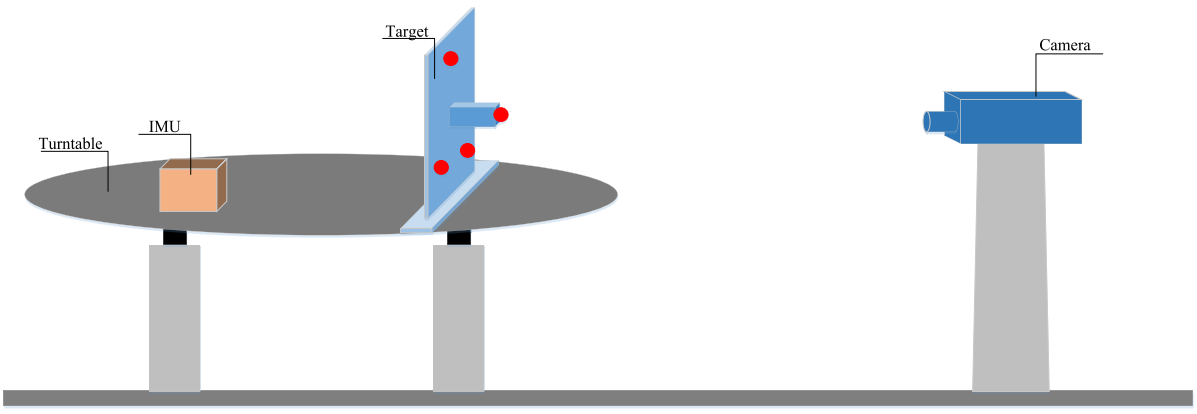

FIGURE 6. The experimental device setting.

from the built-in gyroscope of IMU and the camera. The used parameters of the built-in gyroscope of IMU are given in Table 1.

A. TIMES SYNCHRONIZATION IN SENSOR FUSION SYSTEM

In order to address the discrepancy between inertial and visual data, the time synchronization is proposed. The program Calculagraph obtains the running time of the system from the beginning. Whenever the gyroscope of IMUS obtains the angular velocity, the time is recorded. Similarly, the time is recorded in the camera as well. The recorded times are aligned in the calculation process by minimizing the difference between two times. As shown in Fig. 7, data from two different sensors are synchronized in the fusion system.

TABLE 1. Parameters of the gyroscope.

	Parameter type	Parameter value
Gyro	In-run bias stability	10 deg/h
	Bandwidth (-3 dB)	450 Hz
	A/D resolution	16 bits
	Noise density	0.01 (deg/s)/√Hz

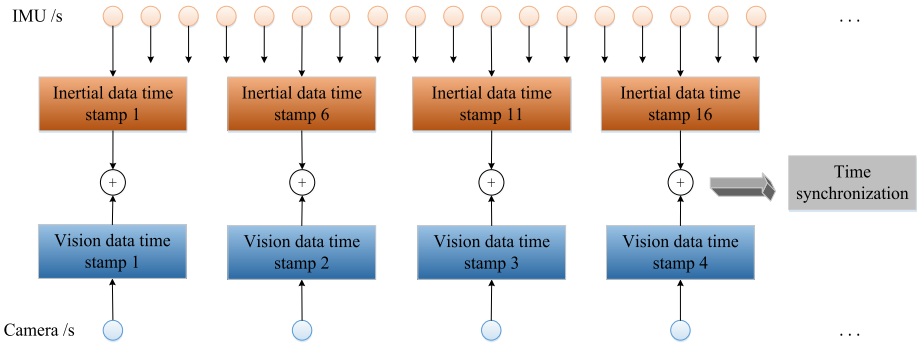

FIGURE 7. Time synchronization of the IMU and camera in the proposed system.

B. COORDINATE SYSTEM NORMALIZATION

In the multi-sensor system for attitude estimation, different sensors have different coordinates. Two different coordinates need to be transformed into the arbitrary coordinate. There are coordinate systems for the arbitrary, camera, IMU, and the target. Fig. 8 describes the normalization across these coordinates.

The relative angles are measured between the body and camera coordinates. The relative coordinate is represented by a rotation matrix $R_c^b(t)$, where t represents time. The coordinate is normalized by transforming inertial and vision measurements to the $R_c^b(t)$. The rotation transformation of inertial and vision quantities from c system to b system is defined as follows.

$$\begin{cases} R_c^b(t) = R_t^b R_c^t(t) \\ R_c^b(t) = R_i^b R_c^i(t), \end{cases} \tag{19}$$

where $R_x^y(t)$ is the rotation matrix from x coordinate to y coordinate. In (19), t and i indicate the vision sensor and the inertial sensor, respectively. Since the target and IMU are fixed, R_t^b and R_i^b can be computed by calibration.

The rotation transformation between two coordinates is described by triple rotation parameters along x, y, and z axes, which correspond to α, β and θ angles. The specific conversion process is shown in Fig. 9.

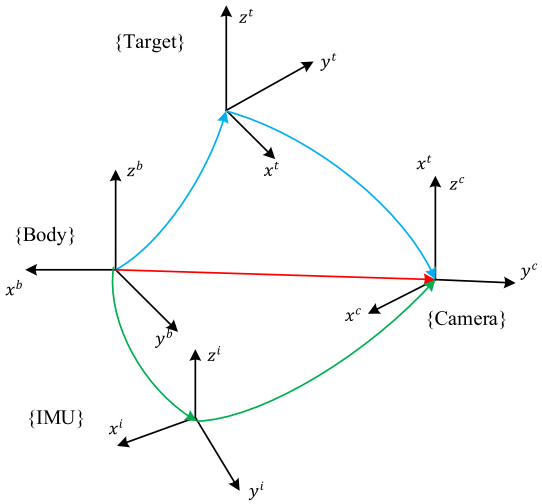

FIGURE 8. Coordinates transformation across different sensors.

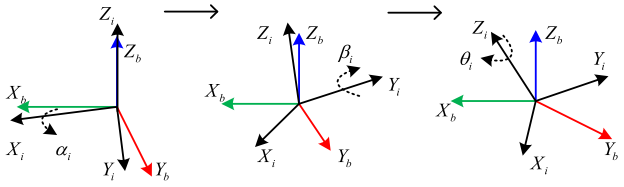

FIGURE 9. The rotation transformation of two coordinate system.

C. COMPARISON WITH OTHER METHODS ON REPEATED EXPERIMENTS

The performance of the proposed MLP-CKF is compared with other methods: EKF, CKF, and backpropagation CKF (BP-CKF). We designed the motion trajectory of an object, named as round-trip-step-up motion. Fig. 10 shows the trajectory where the pitch and yaw angles vary from -20 degrees to +20 degrees in round-trip and step-up forms, respectively.

The errors of the attitude angle in the pitch and yaw angles are plotted in Fig. 11. In the proposed method, LWLR fits the visual data in 0s∼10s and 40s∼50s to get the fitted visual

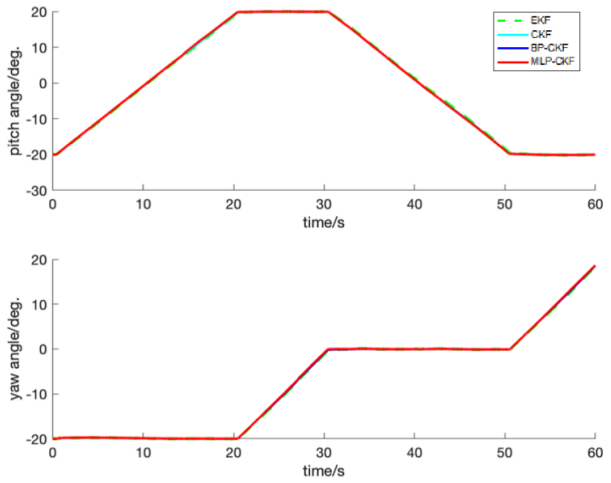

FIGURE 10. Round-trip-step-up motion. Top: pitch angle, bottom: yaw angle.

data in pitch angle, while in 20s∼30s and 60s∼70s to get the fitted visual data in yaw angle. Then, the obtained four fitted vision data are used to predict the next ten seconds of each fitted vision data. The four groups of predicted vision data and the corresponding actual vision data are subtracted, then the vision data errors are calculated. When the vision data is accessible, MLP is used for training the vision data errors and establish the training model. During the interval of sampling in vision data, the MLP model is employed to estimate the vision errors. Then, inertial data from gyroscope are corrected by MLP estimated vision result to compute final attitude angles.

As shown in Fig. 11, the proposed MLP-CKF outperforms the EKF, CKF, and BP-CKF in terms of stability and accuracy. The proposed MLP-CKF shows remarkable performance, especially during the period of 25s-35s, 55s-65s for the yaw axis and the 15s-25s, 45s-55s for the pitch axis. More importantly, it indicates that the MLP-CKF algorithm converges better during the interval of invalid vision data.

When visual measurements are available, compared methods estimate the attitude by fusing inertial and visual data. In contrast, when the visual data is unavailable, EKF and CKF estimate the attitude by using inertial data only. BP-CKF estimates the attitude by using inertial data compensated by BP prediction results. Then, it is combined with CKF, providing the estimated attitudes. In the proposed MLP-CKF, the attitude angles are computed from inertial data. Then, the attitude angles are compensated by MLP that is predicted vision results, estimating the final attitudes. The optimal estimation of MLP-CKF leads to superior performance over the three compared methods. Table 2 and Fig. 12 present a quantitative evaluation of the proposed method with the compared methods in terms of Maximum errors and Root Mean Squared Error (RMSE). The results show that MLP-CKF is more stable than the comparison methods.

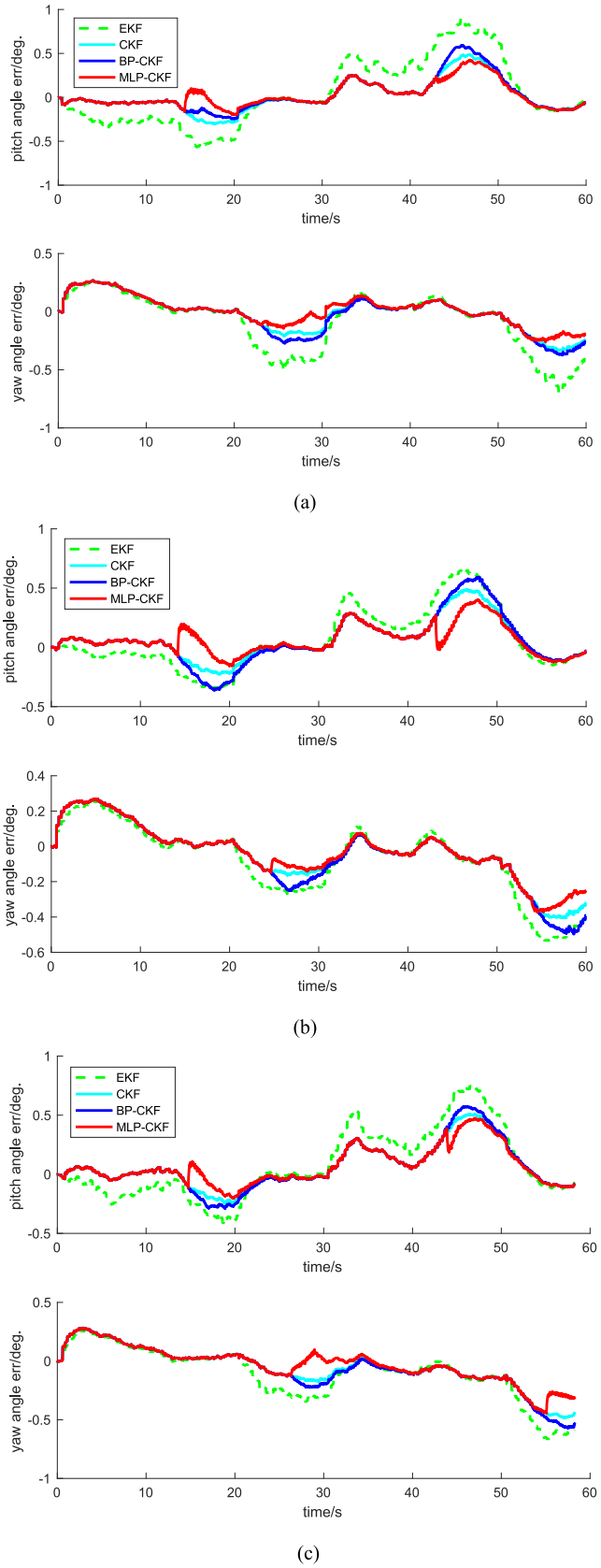

FIGURE 11. The attitude errors in the repeated experiments (a)-(c).

TABLE 2. Max error and RMSE of three groups experiment.

	pitch		yaw	
	Max Error	RMSE	Max Error	RMSE
EKF-1	0.9039	0.3515	-0.7013	0.2783
CKF-1	0.4784	0.1163	-0.3375	0.1233
BP-CKF-1	0.4795	0.2473	-0.3731	0.2531
MLP-CKF-1	0.3829	0.0532	-0.2464	0.0658
EKF-2	0.6617	0.2451	-0.5378	0.1785
CKF-2	0.4519	0.1055	-0.4187	0.1509
BP-CKF-2	0.5373	0.2501	-0.4821	0.1615
MLP-CKF-2	0.4035	0.0471	-0.3373	0.1265
EKF-3	0.7494	0.3438	-0.6702	0.2254
CKF-3	0.5035	0.1216	-0.4718	0.1801
BP-CKF-3	0.5932	0.2478	-0.5852	0.2017
MLP-CKF-3	0.3170	0.0769	-0.4043	0.1376

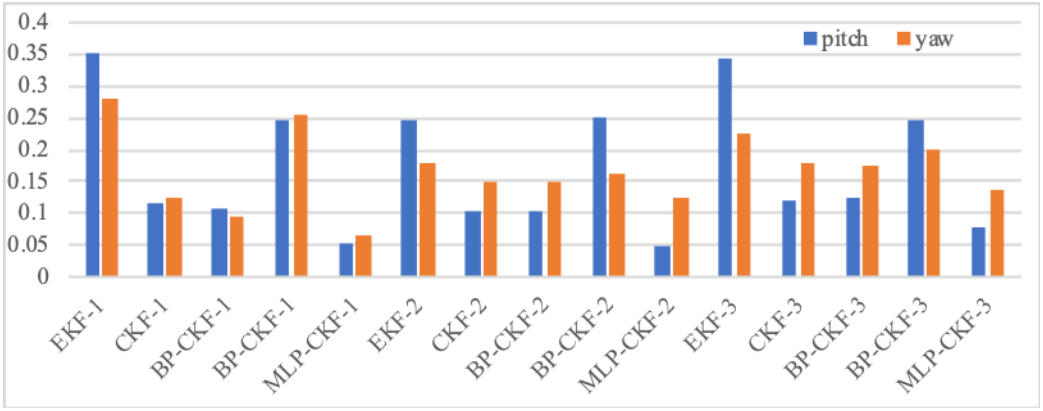

FIGURE 12. RMSE comparison of three groups of experiments.

IV. CONCLUSION

An enhanced strategy for multi-frequency data fusion is proposed based on MLP and CKF. The strategy improves the attitude estimation of inertial and vision data by considering the discrepancy of sampling-frequency and the filtering divergence. The proposed method not only mitigates the divergence problem in the interval of invalid vision data but also guarantees the stable high-frequency attitude angles. Unlike the existing methods, the predicted vision error is compensated for the unstable inertial data when the vision data is unavailable, and the present scheme fully utilizes the past inertial and vision information. Experimental results under different scenarios show that the proposed method reliably estimates the attitude and achieves the enhanced convergence capability. In future work, the influences of long motion trajectory and larger variation of tilt angles on the system will be invesgated.

REFERENCES

[1] N. Enayati, E. De Momi, and G. Ferrigno, "A quaternion-based unscented Kalman filter for robust optical/inertial motion tracking in computer-assisted surgery," *IEEE Trans. Instrum. Meas.*, vol. 64, no. 8, pp. 2291–2301, Aug. 2015.

[2] N. Li, L. Zhao, L. Li, and C. Jia, "Integrity monitoring of high-accuracy GNSS-based attitude determination," *GPS Solutions*, vol. 22, no. 4, p. 22, Oct. 2018.

[3] H. No, A. Cho, and C. Kee, "Attitude estimation method for small UAV under accelerative environment," *GPS Solutions*, vol. 19, no. 3, pp. 343–355, Jul. 2015.

[4] H. Himberg, Y. Motai, and A. Bradley, "A multiple model approach to track head orientation with delta quaternions," *IEEE Trans. Cybern.*, vol. 43, no. 1, pp. 90–101, Feb. 2013.

[5] J. Jin, L. N. Zhao, and S. L. Xu, "High-precision rotation angle measurement method based on monocular vision," *J. Opt. Soc. Amer.*, vol. 31, pp. 1401–1407, Jul. 2014.

[6] Y. Rong, Q. Wang, S. Lu, G. Li, Y. Lu, and J. Xu, "Improving attitude detection performance for spherical motors using a MEMS inertial measurement sensor," *IET Electr. Power Appl.*, vol. 13, no. 2, pp. 198–205, Feb. 2019.

[7] J. Yu, X. Z. Bu, C. Xiang, and X. Z. Wang, "Spinning projectile's attitude measurement using background magnetic field compensation," *J. Appl. Remote Sens.*, vol. 2016, 10, 014001.

[8] X. Guo, J. Tang, J. Li, C. Shen, and J. Liu, "Attitude measurement based on imaging ray tracking model and orthographic projection with iteration algorithm," *ISA Trans.*, vol. 95, pp. 379–391, Dec. 2019.

[9] S. Zhou, F. Fei, G. Zhang, Y. Liu, and W. Li, "Hand-writing motion tracking with vision-inertial sensor fusion: Calibration and error correction," *Sensors*, vol. 14, no. 9, pp. 15641–15657, Aug. 2014, doi: 10.3390/s140915641.

[10] J. Li, "Binocular vision measurement method for relative position and attitude based on dual-quaternion," *J. Mod. Opt.*, vol. 64, pp. 1846–1853, Oct. 2017.

[11] C. G. Park, C. H. Kang, S. Hwang, and C. J. Chung, "An adaptive complementary filter for gyroscope/vision integrated attitude estimation," *Int. J. Aeronaut. Space Sci.*, vol. 17, no. 2, pp. 214–221, Jun. 2016.
[12] C. Shen, J. Yang, J. Tang, J. Liu, and H. Cao, "Note: Parallel processing algorithm of temperature and noise error for micro-electro-mechanical system gyroscope based on variational mode decomposition and augmented nonlinear differentiator," *Rev. Sci. Instrum.*, vol. 89, no. 7, Jul. 2018, Art. no. 076107.
[13] S. Chong, S. Rui, L. Jie, Z. Xiaoming, T. Jun, S. Yunbo, L. Jun, and C. Huiliang, "Temperature drift modeling of MEMS gyroscope based on genetic-elman neural network," *Mech. Syst. Signal Process.*, vols. 72–73, pp. 897–905, May 2016.
[14] C. Shen, X. Liu, H. Cao, Y. Zhou, J. Liu, J. Tang, X. Guo, H. Huang, and X. Chen, "Brain-like navigation scheme based on MEMS-INS and place recognition," *Appl. Sci.*, vol. 9, no. 8, p. 1708, Apr. 2019.
[15] H. Gui and A. H. J. de Ruiter, "Quaternion invariant extended Kalman filtering for spacecraft attitude estimation," *J. Guid., Control, Dyn.*, vol. 41, no. 4, pp. 863–878, Apr. 2018.
[16] D. Lee, G. Vukovich, and R. Lee, "Robust adaptive unscented Kalman filter for spacecraft attitude estimation using quaternion measurements," *J. Aerosp. Eng.*, vol. 30, no. 4, Jul. 2017, Art. no. 04017009.
[17] C. Shen, Y. Zhang, J. Tang, H. Cao, and J. Liu, "Dual-optimization for a MEMS-INS/GPS system during GPS outages based on the cubature Kalman filter and neural networks," *Mech. Syst. Signal Process.*, vol. 133, Nov. 2019, Art. no. 106222.
[18] X. Li and W. Zhang, "Reliable integrated navigation system based on adaptive fuzzy federated Kalman filter for automated vehicles," *Proc. Inst. Mech. Eng., D, J. Automobile Eng.*, vol. 224, no. 3, pp. 327–346, Mar. 2010.
[19] F. Yang, Y. Luo, and L. Zheng, "Double-layer cubature Kalman filter for nonlinear estimation," *Sensors*, vol. 19, no. 5, p. 986, Feb. 2019.
[20] C. Shen, Y. Zhang, X. Guo, X. Chen, H. Cao, J. Tang, J. Li, and J. Liu, "Seamless GPS/inertial navigation system based on self-learning square-root cubature Kalman filter," *IEEE Trans. Ind. Electron.*, early access, Jan. 23, 2020, doi: 10.1109/TIE.2020.2967671.
[21] J. Zhang, J. Cao, and D. Zhang, "ANN-based data fusion for lumber moisture content sensors," *Trans. Inst. Meas. Control*, vol. 28, pp. 69–79, Mar. 2006.
[22] L. Zhao, N. Li, L. Li, Y. Zhang, and C. Cheng, "Real-time GNSS-based attitude determination in the measurement domain," *Sensors*, vol. 17, no. 2, p. 296, Feb. 2017, doi: 10.3390/s17020296.
[23] D. Cilden, H. E. Soken, and C. Hajiyev, "Nanosatellite attitude estimation from vector measurements using SVD-aided UKF algorithm," *Metrology Meas. Syst.*, vol. 24, no. 1, pp. 113–125, Mar. 2017.
[24] G. Jiang, L. Liu, C. Guo, J. Chen, F. Muhammad, and X. Miao, "A novel fusion algorithm for estimation of the side-slip angle and the roll angle of a vehicle with optimized key parameters," *Proc. Inst. Mech. Eng., D, J. Automobile Eng.*, vol. 231, no. 2, pp. 161–174, Feb. 2017.
[25] X. Guo, J. Tang, J. Li, C. Wang, C. Shen, and J. Liu, "Determine turntable coordinate system considering its non-orthogonality," *Rev. Sci. Instrum.*, vol. 90, no. 3, Mar. 2019, Art. no. 033704.